The Soluble Wnt Receptor Frizzled8CRD-hFc Inhibits the Growth of Teratocarcinomas *In vivo*

Venita I. DeAlmeida,[1] Li Miao,[1] James A. Ernst,[2] Hartmut Koeppen,[3] Paul Polakis,[1] and Bonnee Rubinfeld[1]

Departments of [1]Cancer Pathways and Targets, [2]Protein Chemistry and Protein Engineering, and [3]Pathology, Genentech Inc., South San Francisco, California

Abstract

Wnt signaling is important for normal cell proliferation and differentiation, and mutations in pathway components are associated with human cancers. Recent studies suggest that altered wnt ligand/receptor interactions might also contribute to human tumorigenesis. Therefore, agents that antagonize wnt signaling at the extracellular level would be attractive therapeutics for these cancers. We have generated a soluble wnt receptor comprising the Frizzled8 cysteine-rich domain (CRD) fused to the human Fc domain (F8CRDhFc) that exhibits favorable pharmacologic properties *in vivo*. Potent antitumor efficacy was shown using the mouse mammary tumor virus-Wnt1 tumor model under dosing conditions that did not produce detectable toxicity in regenerating tissue compartments. *In vitro*, F8CRDhFc inhibited autocrine wnt signaling in the teratoma cell lines PA-1, NTera-2, Tera-2, and NCCIT. *In vivo*, systemic administration of F8CRDhFc significantly retarded the growth of tumor xenografts derived from two of these cell lines, PA-1 and NTera-2. Pharmacodynamic markers of wnt signaling, identified by gene expression analysis of cultured teratoma cells, were also modulated in the tumor xenografts following treatment with F8CRDhFc. Additionally, these markers could be used as indicators of treatment efficacy and might also be useful in identifying patients that would benefit from the therapeutic agent. This is the first report showing the efficacy of a soluble wnt receptor as an antitumor agent and suggests that further development of wnt antagonists will have utility in treating human cancer. [Cancer Res 2007;67(11):5371–9]

Introduction

Wnt signaling is a complex process involving several cell surface receptors and intracellular intermediates (1, 2). The wnt pathway is activated by the binding of wnt ligands to two classes of cell surface receptors, the Frizzleds (Fzd) and the low-density lipoprotein receptor–related proteins, LRP5 and LRP6. The resulting signaling cascade leads to the stabilization and nuclear translocation of β-catenin, the key effector molecule of the wnt pathway. Wnt signaling is a critical regulator of cell fate during differentiation and development of the embryo (3). In adults, wnt signaling regulates self-renewal and regeneration of tissues such as skin, intestine, and hematopoietic cells, through processes dependent on stem cell function (4).

The wnt pathway was originally implicated in tumorigenesis with the observation that activation of the *wnt-1* gene by insertion of the mouse mammary tumor virus (MMTV) resulted in mammary gland tumor formation in mice (5, 6). Since then, several studies have shown a role for the wnt pathway in human tumors (7, 8) and experimental cancer models (9, 10). The strongest evidence for a causal role of the wnt pathway in human cancer development comes from extensive studies showing that intracellular wnt signaling intermediates are mutated in different human tumors (7, 8, 11). These include inactivating mutations and hypermethylation of the *APC* gene, activating mutations in the *β-catenin* gene, and inactivating mutations in the *Axin* genes. Mutational activation of wnt signaling in cancer culminates with hyperactivation of TCF/LEF transcription factors through their interaction with β-catenin. The wnt signaling pathway also regulates the expression of genes that control cell proliferation, angiogenesis, resistance to apoptosis, and tissue invasion, and thus, directly plays a role in tumor development and progression (7, 8).

In recent years, there has been increasing evidence that altered expression of wnt ligands, receptors, and extracellular antagonists might be associated with human cancer development and progression. *Wnt* genes are overexpressed in tumor samples (12, 13) and autocrine signaling by wnt ligands has been reported in human cancer cell lines (14, 15). Expression of the fzd receptors (12, 16) and LRP5 (17) is increased in some cancers, whereas overexpression of LRP6 increases tumor cell growth *in vivo* (18). Additionally, genes for the secreted wnt antagonists Wnt inhibitory factor-1 (WIF-1; ref. 19), secreted Frizzled-related proteins (sFRP; refs. 20, 21) and Dickkopf proteins (Dkk; ref. 22) are down-regulated or inactivated in human cancers. WIF-1 and sFRPs directly bind wnt ligands and inhibit their interaction with the fzd receptors, whereas Dkk1 binds the wnt coreceptors LRP5/6 and cause their internalization and degradation (23).

The role of altered wnt signaling at the receptor-ligand level in human tumorigenesis is further strengthened by reports that extracellular wnt antagonists display antitumor activity *in vivo*. Treatment with anti-wnt antibodies (24, 25) and transfection of cDNAs encoding wnt inhibitors such as the cysteine-rich domain (CRD) of fzd7 (26), sFRP1 (14), sFRP3 (27), and a dominant-negative form of LRP5 (27) reduces tumor growth in various *in vivo* models. In this study, we have explored the pharmacologic utility of a soluble wnt receptor that inhibits wnt signaling as an antitumor agent. Our results provide direct evidence that specific extracellular antagonists of wnt signaling can reduce tumor growth and have potential use as anticancer therapeutics.

Note: Supplementary data for this article are available at Cancer Research Online (http://cancerres.aacrjournals.org/).

Requests for reprints: Bonnee Rubinfeld, Cancer Pathways and Targets, Genentech, Inc., 1 DNA Way, MS 40, South San Francisco, CA 94080. Phone: 650-225-5649; Fax: 650-225-6443; E-mail: bonrubin@gene.com.

doi:10.1158/0008-5472.CAN-07-0266

Materials and Methods

Generation of Fzd8CRD expression constructs. The cDNA for murine residues 1–173 of Fzd8 was cloned by PCR, and the cDNA encoding residues 1–155 and 1–173 were subcloned into a pRK-derived plasmid for mammalian expression. In both constructs, the NH_2-terminal CRD of Fzd8 was fused to the human IgG (hFc) effector domain (28) via a short linker region including the residues Leu-Ser-Gly-Gly-Gly-Gly-Val-Thr, to create the Fzd8-hFc fusion construct. The amino acid sequences of murine and human Fzd8 were identical over this region.

Protein isolation and analysis. The human CD4 protein fused to the human IgG domain was used as a nonspecific control protein (29) for all *in vivo* and *in vitro* studies. The wnt3a protein used for *in vitro* assays was purified from L cells transfected with mouse wnt3a (American Type Culture Collection) as previously described (30).

The Fzd8(1–173)hFc and F8CRDhFc proteins were expressed in transiently transfected Chinese hamster ovary cells and isolated by affinity capture using ProSep (Millipore) protein A–conjugated resin. Higher order aggregates were separated from dimers by gel-filtration over a Superdex 200 column (GE Healthcare). Protein identity and NH_2-terminal sequences of the proteins were confirmed by Edmund degradation. SDS-PAGE analysis showed that the F8CRDhFc protein was >95% pure with no significant degradation and with endotoxin levels <1.0 EU/mg (data not shown). Multi-angle laser light scattering showed the protein to be monodispersed with a molecular weight of 95 kDa (data not shown).

BIAcore analysis of wnt3a binding to F8CRDhFc was carried out using immobilized F8CRDhFc and injecting wnt3a as previously described (31). F8CRDhFc protein was amine-coupled to a Biacore CM5 sensor chip (BIAcore, Inc.) to achieve ~9,000 response units of coupled protein. Purified human wnt3a was injected at 0.5 μg/mL and binding assessed by the change in response units as a function of time. *Escherichia coli*–expressed wnt3a was used as a negative control for binding. All procedures after protein immobilization were conducted in PBS with 1 mmol/L of $CaCl_2$ and 1% CHAPS.

Mammalian cell culture, transfection, and luciferase assays. Human kidney epithelial 293 (HEK293) cells and human ovarian PA-1 cells were grown in 50:50 high-glucose DMEM and Ham's F12 with 10% fetal bovine serum (FBS). Human teratoma–derived NTera-2 and Tera-2 cells were maintained in McCoy's medium with 15% FBS, whereas NCCIT cells were maintained in RPMI with 10% FBS.

For luciferase assay transfections, 5×10^5 HEK293 and 1×10^5 PA-1, NCCIT, NTera-2, or Tera-2 cells were plated per well of a 12-well dish (Nunc) 24 h before transfections. Cells were transfected with 0.375 μg of TOPglow (Upstate), 0.10 μg of LEF1, and 0.01 μg of SV40 RL with Fugene (Roche). After 24 h, the medium was changed and cells were left untreated or treated with purified wnt3a at 100 to 300 ng/mL, with the indicated proteins at 2.5 to 5 μg/mL, or with a 1:100 dilution of serum samples for an additional 20 to 24 h before harvesting. Cells were harvested in 50 to 100 μL of lysis buffer [20 mmol/L Tris (pH 8.0), 137 mmol/L NaCl, 1 mmol/L EGTA, 1% Triton X-100, 10% glycerol, 1.5 mmol/L $MgCl_2$, 1 mmol/L DTT, 50 mmol/L NaF, 1 mmol/L $NaVO_4$, and protease inhibitors] and 10 μL samples were assayed in duplicate using Dual-Glo Luciferase assay (Promega) and detected in an Envision Luminometer (Perkin-Elmer). Luciferase activity was normalized against *Renilla* luciferase activity.

Animals. Female athymic nude (*nu/nu*) mice 6 to 8 weeks old (Charles River Laboratories) were used for pharmacodynamic and *in vivo* efficacy studies, whereas female C57Bl6 mice (The Jackson Laboratory) were used for the passaging of MMTV-Wnt1 tumors. Maintenance of mice and *in vivo* procedures were carried out using Institutional Animal Care and Use Committee–approved protocols.

Determination of *in vivo* stability and pharmacodynamics. Four groups of female athymic nude mice (12 animals/group) were given F8CRDhFc as follows: (*a*) F8CRDhFc 1 mg/kg i.v., (*b*) F8CRDhFc 5 mg/kg i.v., (*c*) F8CRDhFc 20 mg/kg i.v., (*d*) F8CRDhFc 20 mg/kg i.p. At various time points, 125 μL of blood was collected from three different animals by retroorbital bleed and the concentration of F8CRDhFc in serum was determined by ELISA. Three hundred and eighty-four–well plates (Nunc Maxisorp) were coated overnight with 1 μg/mL of rabbit anti-human IgG (Jackson ImmunoResearch) in PBS. The plates were blocked with PBS containing 0.5% bovine serum albumin and 10 ppm proclin and washed with assay/wash buffer (PBS, 0.05% Tween 20 and 10 ppm proclin). The F8CRDhFc standards and the diluted serum samples were incubated for 2 h at room temperature and bound F8CRDhFc was detected using horseradish peroxidase goat anti-human IgG (Jackson ImmunoResearch) and the HRP substrate TMB (Moss, Inc.). Concentrations of F8CRDhFc in serum samples were determined using a standard curve fit to a four-parameter algorithm.

For immunoblot detection of Fc-tagged proteins in serum, 1 μL of serum was electrophoresed on 10% SDS-PAGE gels, detected with anti-human IR-conjugated antibody (Rockland Immunochemicals), and scanned on the Odyssey Infrared Imaging System (Li-Cor).

Passaging of MMTV-Wnt1 transgenic tumors in mice. The tumors from MMTV-Wnt1 transgenic mice were serially passaged in C57Bl6 mice for 6 to 10 passages by surgical implantation in the mammary fat pad. Tumor tissue was aseptically collected from the transgenic mouse, rinsed in HBSS and cut into small pieces. The recipient mice were anaesthetized with a mixture of ketamine (75–80 mg/kg) and xylazine (7.5–15 mg/kg), the tumor fragment inserted under the skin rostral to the third mammary fat pad, and the skin closed using wound clips. Tumors were passaged for a maximum of 10 passages, and after the first two passages, tumor tissue was examined histologically to confirm that it was of mammary origin.

***In vivo* efficacy studies.** For *in vivo* efficacy studies in the MMTV-Wnt1 tumor model, tissue from serially passaged MMTV-Wnt1 tumors was macerated in HBSS and the cells obtained were used for allografts. For *in vivo* studies using the NTera-2 or PA-1 model systems, either 8 million NTera-2 cells per mouse or 10 million PA-1 cells per mouse were inoculated. All cells were suspended in a 50% Matrigel solution in HBSS and a volume of 0.2 mL was injected s.c. into the right dorsal flank of athymic nude mice.

After 5 to 12 days of cell inoculation, tumor measurements and grouping of mice was done as previously described (32). Treatments were started 1 to 2 days after grouping and therapeutic agents were dosed by either i.p. or i.v. route with 100 to 200 μL of protein or vehicle (PBS). For all studies, the mice were treated with a single loading dose of 15 mg/kg, followed by subsequent doses at 10 mg/kg. Frequency and length of treatments are indicated for each study. Tumor volume was measured twice weekly and animals were sacrificed when tumor volume reached 2,500 mm^3 or when tumors showed signs of impending ulceration. Data collected from each experimental group were expressed as mean ± SEM and the statistical significance of efficacy was assessed by Student's *t* tests (two-tailed distribution, two-sample unequal variance).

Preparation and analysis of RNA from cell lines and tumor tissue. For microarray analysis, cells were treated with the indicated proteins in triplicate and total RNA was isolated using the RNAeasy kit (Qiagen). Array analysis was done on the Affymetrix Human Genome U133 Gene Chip set as previously described (32).

Tumor tissue RNA was purified from xenograft specimens collected at the end of the efficacy study and quantitative reverse transcription-PCR (qRT-PCR) analysis of wnt-responsive transcripts carried out as previously described (32). Fold induction for each gene was determined using the ΔΔCt method and the result presented relative to glyceraldehyde-3-phosphate dehydrogenase. The specific probes and primer sets are listed in Supplementary Table S1. All reactions were done in duplicate and the average of at least two assays ± SEM was plotted.

Histology and immunohistochemistry on formalin-fixed paraffin-embedded tissues. Immunohistochemistry for β-catenin was done on tumor xenograft tissue, skin and intestine harvested at the termination of efficacy studies. Tissues were formalin-fixed, paraffin-embedded, and serial sections were subjected to antigen retrieval (Dako Target Retrieval), following which β-catenin was detected with a monoclonal antibody (clone 14; BD PharMingen) as previously described (33). The sections were counterstained with hematoxylin (Vector Lab) and mounted using Histomount (Zymed).

Results

Activity, stability, and pharmacokinetics of F8CRDhFc. Purified Fzd8(1–173)hFc was previously shown to effectively inhibit wnt signaling *in vitro* (34, 35). Prior to testing the antitumor efficacy of Fzd8(1–173)hFc, we determined the half-life of this protein and found that it was rapidly cleared *in vivo*. Using data from the crystal structure of the mouse Fzd8 domain (36), we generated a minimal Fzd8 construct in which potential protease cleavage sites were deleted (Fig. 1*A*). This protein, denoted as F8CRDhFc, consists of residues 1–155 of the Fzd8 receptor fused to the hFc domain. Using BIAcore analysis, we determined that F8CRDhFc directly binds wnt3a purified from L cells (Fig. 1*B*), but not wnt3a purified from *E. coli* (data not shown), which is inactive due to the lack of lipid modification (30). Kinetic binding data for this interaction could not be approximated using simple binding models, possibly due to the dimeric nature of F8CRDhFc (data not shown). F8CRDhFc also inhibited TOPflash reporter signaling in wnt3a-stimulated U2OS cells in a dose-dependent manner with an apparent IC_{50} of 1 to 2 nmol/L (Supplementary Fig. S1), suggesting that the molecule was active at low concentrations.

The stability of F8CRDhFc protein *in vivo* was determined by assaying both protein levels and activity in serum collected at various time points from animals injected i.v. with 10 mg/kg of protein. Using Western blot analysis, F8CRDhFc was detectable in serum 72 h after administration, whereas Fzd8(1–173)hFc was not detectable beyond 30 min (Fig. 1*C, inset*). The activity of F8CRDhFc in the collected serum was assayed by measuring the inhibition of wnt3a-dependent TOPglow reporter activity in HEK293 cells. Although comparable *in vitro* potency was observed on treatment with purified Fzd8(1–173)hFc and F8CRDhFc at 2.5 μg/mL, only partial inhibitory activity was recovered from the serum of Fzd8(1–173)hFc-treated mice collected 30 min after protein administration. In contrast, more potent inhibitory activity could be recovered from the serum of F8CRDhFc-treated mice for up to 24 h after administration (Fig. 1*C*). Therefore, F8CRDhFc protein was used for all subsequent studies.

We tested the *in vivo* pharmacokinetics of F8CRDhFc by administration of a single dose of protein at 1, 5, or 20 mg/kg i.v. or at 20 mg/kg i.p. Following both i.v. and i.p. administration, F8CRDhFc displayed a dose-proportional increase in exposure with biphasic elimination at all doses (Fig. 1*D*). When dosed at 20 mg/kg

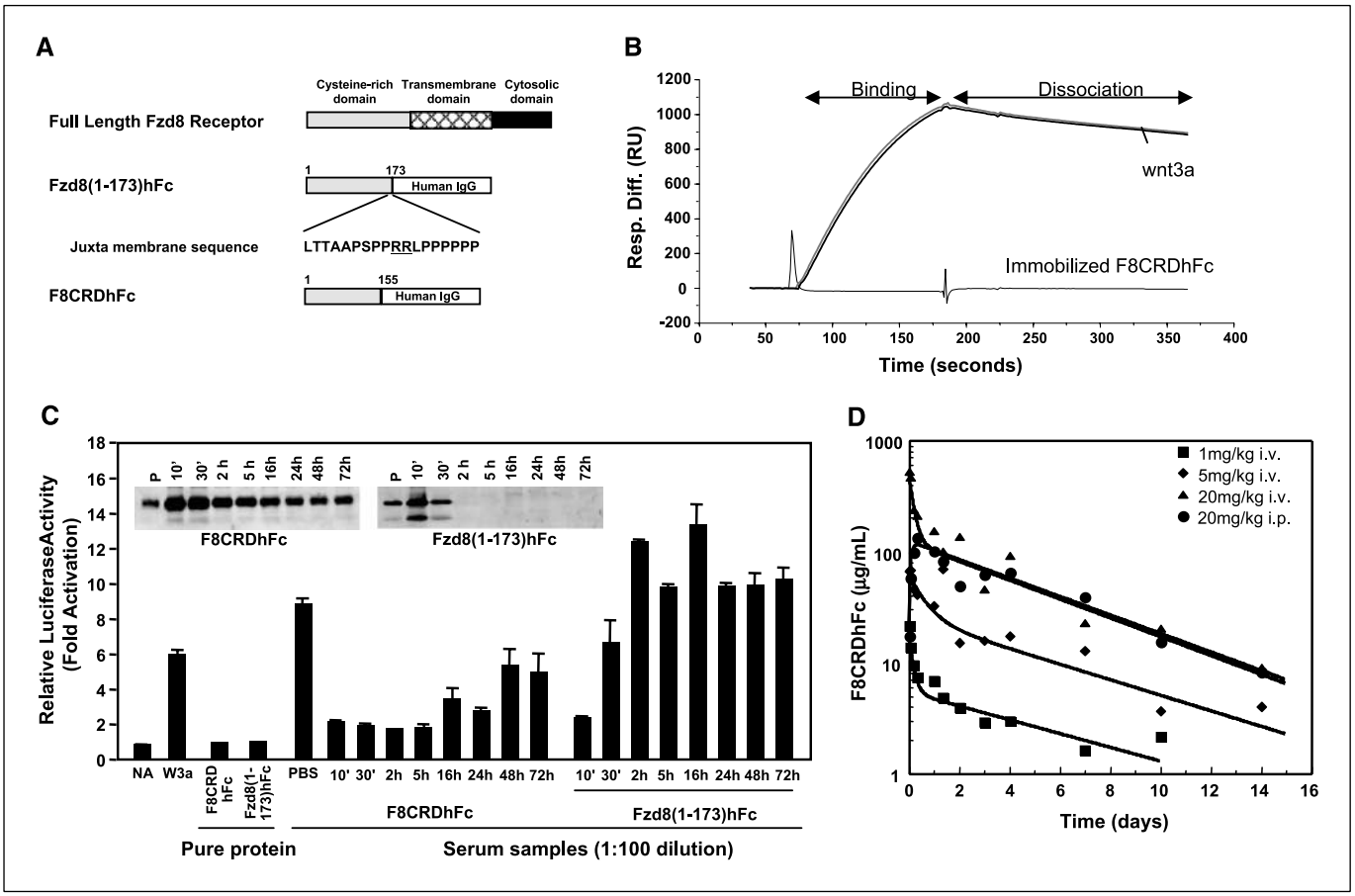

Figure 1. Generation and characterization of F8CRDhFc. *A,* extracellular domain residues 1–173 of Fzd8 were fused to the Fc region of a human immunoglobulin domain to produce Fzd8(1–173)hFc. Amino acid residues 156–173 of Fzd8 contain a flexible juxtamembrane domain with putative protease cleavage sites that were removed to produce F8CRDhFc. *B,* BIAcore sensogram generated by binding purified soluble wnt3a to immobilized F8CRDhFc. The traces represent two individual experiments done under identical conditions. *C,* athymic nude mice were injected i.v. with 10 mg/kg of either Fzd8(1–173)CRDhFc or F8CRDhFc and serum collected at the indicated time points was analyzed for total and active protein. Immunoblotting for human Fc (*top*) was used to detect the protein present in 1 μL of serum and compared with 25 μg of the respective purified protein (*P*). Wnt inhibitory activity was assayed by measuring TOPglow activity in wnt3a-stimulated HEK293 cells treated with serum of injected animals (*bottom right*). Antagonist activity of purified Fzd8(1–173)hFc and F8CRDhFc in HEK293 cells is also shown (*bottom left*). The TOPglow activity in treated cells is represented as fold induction relative to cells that were not treated with either antagonist or wnt3a (*NA*). *D*, serum levels of F8CRDhFc following administration of a single dose of protein. Mice were dosed at either 1, 5, or 20 mg/kg i.v. or 20 mg/kg i.p. and serum samples were taken from individual mice at the indicated time points. The levels of F8CRDhFc in serum were determined by ELISA; *points,* averages from three individual mice.

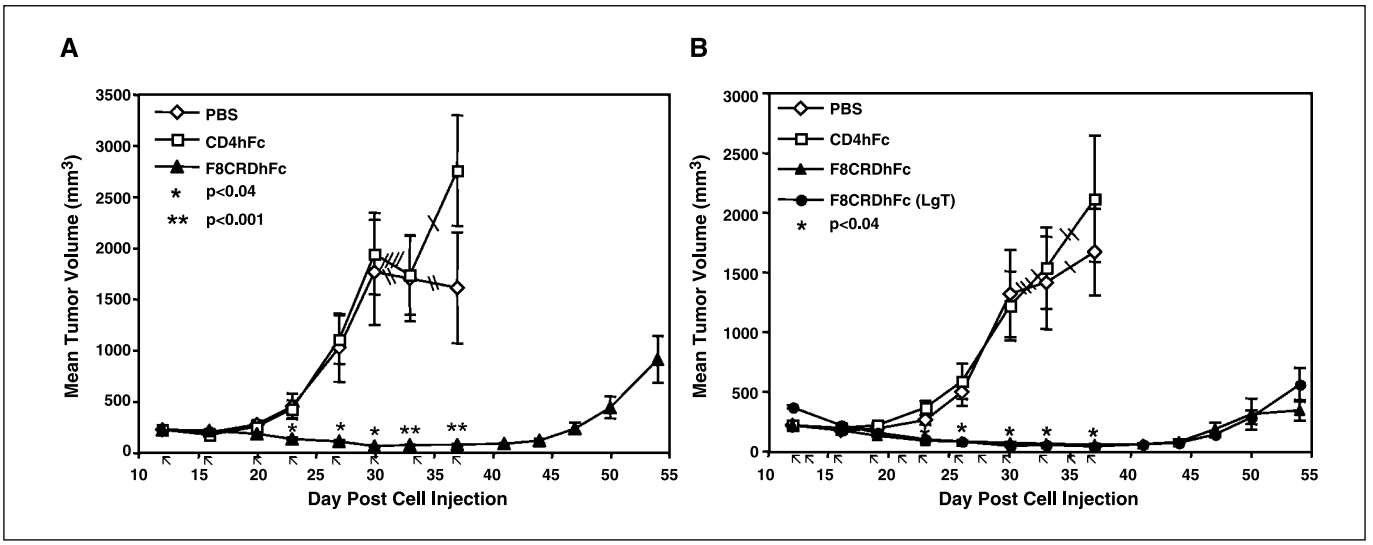

Figure 2. *In vivo* efficacy of F8CRDhFc against MMTV-Wnt1 tumor allografts. Mice bearing established MMTV-Wnt1 tumor transplants were given PBS, CD4hFc (10 mg/kg/d), or F8CRDhFc (10 mg/kg/d) by i.p. injection twice weekly (*A*) or by i.v. injection thrice weekly (*B*). An independent group of mice bearing larger tumors (*LgT*), with a mean tumor volume of 375 mm^3, was also treated in the i.v. experiment. *Points,* mean tumor volume plotted over time; *bars,* SEM; *arrows,* treatment days (*X-axis*); *hatch marks,* sacrificed animals; *asterisks,* statistical significance.

by either the i.p. or i.v. route, comparable serum levels of protein were achieved within a day of injection and the protein was detectable in serum up to 7 days. After i.p. dosing at 20 mg/kg, protein was rapidly absorbed with a T_{max} of ~8 h and bioavailability (AUC_{IP}/AUC_{IV}) of 92%. The clearance of the protein was ~25 to 30 mL/d/kg with a half-life of about 4 days (Supplementary Table S2).

F8CRDhFc inhibits growth of MMTV-Wnt1 tumor allografts. The antitumor efficacy of F8CRDhFc was tested *in vivo* using a model derived from mammary tumors originating in MMTV-Wnt1 transgenic mice (6). Cells isolated from MMTV-Wnt1 tumors were injected into athymic nude mice and, after 12 days, the mice were grouped into seven study groups. Three groups (n = 11) with a mean tumor volume of 226 mm^3 were treated twice weekly with i.p. injections of PBS, F8CRDhFc, or CD4hFc, and three additional groups were treated with the same agents thrice a week by i.v. administration. An additional study group (n = 10), in which the tumors were allowed to reach a larger mean tumor volume of 375 mm^3, was treated with F8CRDhFc i.v. Administration of F8CRDhFc by i.p. or i.v. route resulted in rapid tumor regression with sustained inhibition during the course of treatment, whereas the negative control protein CD4hFc had no effect relative to the PBS treatment (Fig. 2*A* and *B*). The F8CRDhFc-treated mice were followed for 3 weeks after termination of treatments and regrowth of tumors was eventually observed (Fig. 2*A* and *B*).

F8CRDhFc inhibits the growth of human teratoma xenografts. Although inhibition of MMTV-Wnt1 tumor growth shows the pharmacologic activity of F8CRDhFc, inhibition of naturally derived human tumor models would strengthen its potential as a human cancer therapeutic. To identify a relevant model, we tested human tumor–derived cell lines for evidence of autocrine wnt signaling, similar to that seen in the PA-1 teratoma cell line (14). The teratoma-derived NTera-2, Tera-2, and NCCIT cell lines exhibited basal wnt signaling that could be inhibited by F8CRDhFc, contrary to 293 cells that exhibited low basal signaling that was not inhibited by F8CRDhFc (Fig. 3*A*). Nevertheless, all four teratoma cell lines seemed to express wnt receptors, as signaling was further stimulated by wnt3a treatment, which could be blocked by F8CRDhFc (Fig. 3*B*). These results indicate that the teratoma cell lines express wnt(s), which might contribute to their tumorigenicity. We therefore evaluated these lines for tumor formation in athymic nude mice and based on consistency of tumor formation, we selected NTera-2 and PA-1 for *in vivo* efficacy studies.

Six days after inoculation with NTera-2 cells, mice were divided into four treatment groups and treated thrice a week by i.p. administration. Three groups (n = 20), each with a mean tumor volume of 202 mm^3 were treated with PBS, CD4hFc, or F8CRDhFc, whereas a fourth group (n = 10) with a mean tumor volume of 336 mm^3, was treated with F8CRDhFc. Relative to controls, treatment with F8CRDhFc reduced tumor volume and mass by ~50% and 70%, respectively (Fig. 3*C*). We next tested the PA-1 tumor model under similar conditions using three groups of mice (n = 13) harboring tumors with a mean initial volume of 168 mm^3. Again, treatment with F8CRDhFc showed a significant reduction in tumor growth within 12 days of treatment (Fig. 3*D*). In this model, the tumors were ~50% smaller, with significantly smaller mass than those in control groups at the end of the treatment period (Fig. 3*D, inset*).

Wnt target genes as pharmacodynamic markers of drug response. To show that the *in vivo* efficacy observed with F8CRDhFc treatment correlated with inhibition of wnt signaling, we did immunohistochemical analyses for β-catenin localization in tumors of mice treated with F8CRDhFc. Tumors derived from NTera-2, PA-1, NCCIT, and Tera-2 cell lines had varying levels of cytosolic β-catenin with no remarkable nuclear localization (Supplementary Fig. S2). Furthermore, the β-catenin localization pattern was not detectably altered following treatment with F8CRDhFc for 5 or 48 h in MMTV-Wnt1 tumors (data not shown) and NTera-2 tumors (Fig. 4). The small intestine was included as a positive control and nuclear β-catenin was readily detected in the Paneth cells at the base of the crypts. The apparent lack of sensitivity afforded by immunohistochemical analysis of the teratomas prompted us to seek alternative measures for monitoring wnt responsiveness. Although numerous target genes of the wnt pathway have been reported, we did gene expression

analysis on *in vitro*–treated cells to identify those genes most appropriate for the teratoma cells employed in our study. We initially did comparative gene expression analysis on PA-1 cells treated with purified wnt3a, F8CRDhFc, or a control protein. The expression levels of previously identified targets of wnt signaling such as Axin2 (37), APCDD1 (38), and Gad1 (39) were up-regulated by wnt3a treatment or down-regulated by F8CRDhFc treatment (Fig. 5*A*). Moreover, some genes such as Lefty2 (A), Lefty1 (B), sFRP1, and Fzd5 were down-regulated by wnt3a and up-regulated by inhibition of wnt signaling with F8CRDhFc (Fig. 5*A*). Subsequent gene expression analysis by qRT-PCR showed that these transcripts were similarly regulated by wnt3a and F8CRDhFc in NTera-2, Tera-2, and NCCIT cells as well (data not shown).

APCDD1, Gad1, and Fzd5 were among the most consistently modulated genes in our *in vitro* analyses and were therefore selected as potential markers of wnt responsiveness for the *in vivo* tumor xenograft studies. Similar to the effects seen *in vitro*, treatment with therapeutic doses of F8CRDhFc reduced the expression of genes for APCDD1 and Gad1 and increased the expression of Fzd5 in tumors from the NTera-2 xenografts (Fig. 5*B*). Although there is a general nonspecific down-regulation of all genes following CD4hFc treatment, these changes were not statistically significant compared with those seen in F8CRDhFc-treated tumors. These observations show that the antitumorigenic effects of F8CRDhFc *in vivo* are on target and that the expression levels of these genes can be used to monitor the efficacy of potential anti-wnt therapeutic agents.

Therapeutic administration of F8CRDhFc has no adverse effects on regenerating tissue. Wnt signaling plays a critical role in self-renewal of regenerating tissue such as skin, intestine, and hematopoietic cells (4), and inhibition of wnt signaling by Dkk1 can adversely affect the architecture of these tissues in adult mice (35, 40, 41). We therefore determined whether exposure to F8CRDhFc under the same conditions used to obtain antitumor efficacy had any effect on intestine and skin in the mice. Tissues were collected from mice that were treated in the MMTV-Wnt1

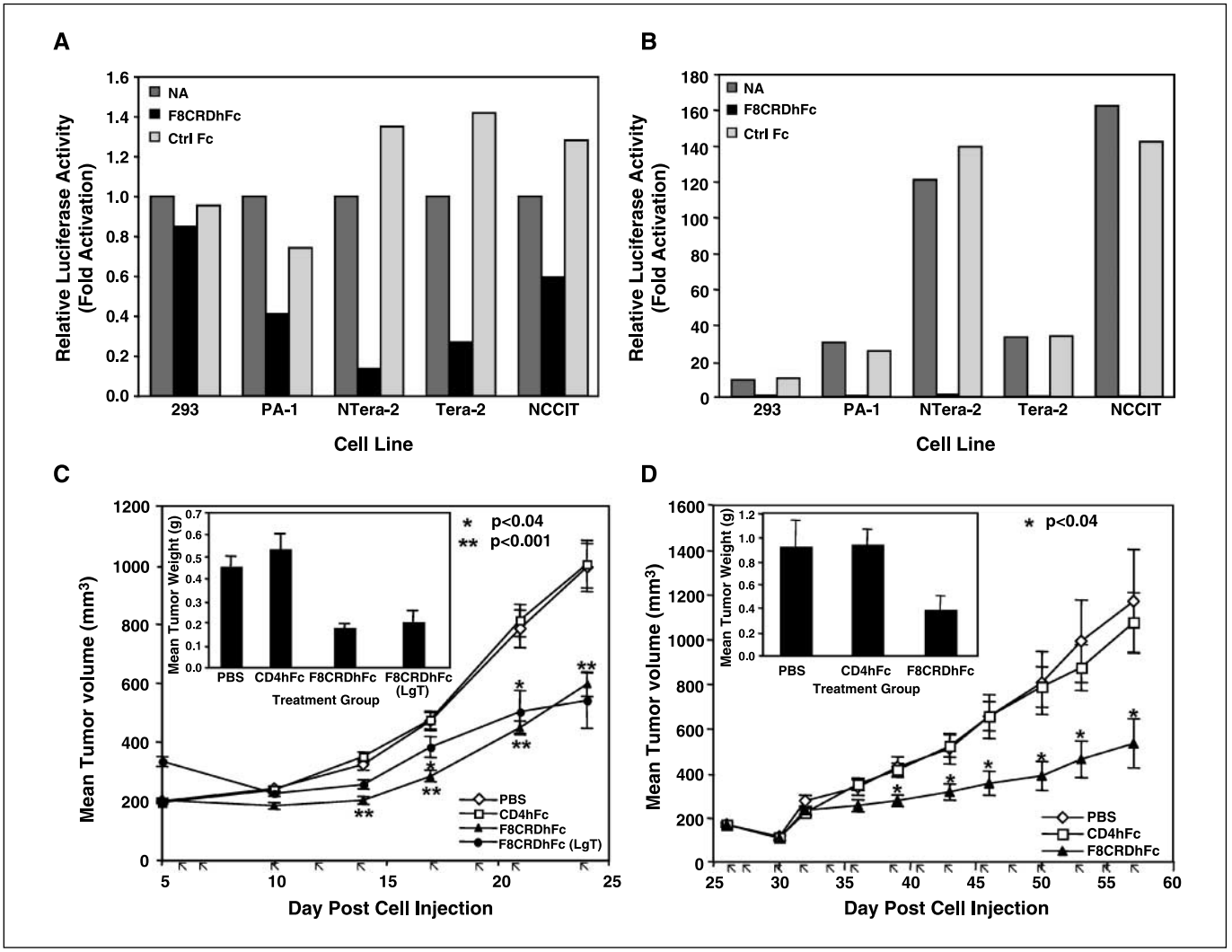

Figure 3. Antitumor efficacy of F8CRDhFc in NTera-2 and PA-1 xenograft tumor models. Relative luciferase activity was measured in the indicated cell lines transfected with the TOPglow plasmid and treated with F8CRDhFc or CD4hFc, in the absence (*A*) or presence (*B*) of exogenously added wnt3a protein. For each cell line, activity was expressed relative to that observed in the absence of any treatment (*NA*); representative of at least two independent experiments. Mice bearing established NTera-2 (*C*) or PA-1 (*D*) tumors were given PBS, CD4hFc (10 mg/kg), or F8CRDhFc (10 mg/kg) by i.p. injection thrice a week. For the NTera-2 tumor study, an independent group of 10 mice with larger tumors (*LgT*) having a mean tumor volume of 336 mm^3 was also tested. *Points,* mean tumor volume plotted over time; *bars,* SEM; *arrows,* treatment days (*X-axis*); *asterisks,* statistical significance. *Columns,* mean tumor weight for each group, determined upon termination of the study; *bars,* SEM (*insets*).

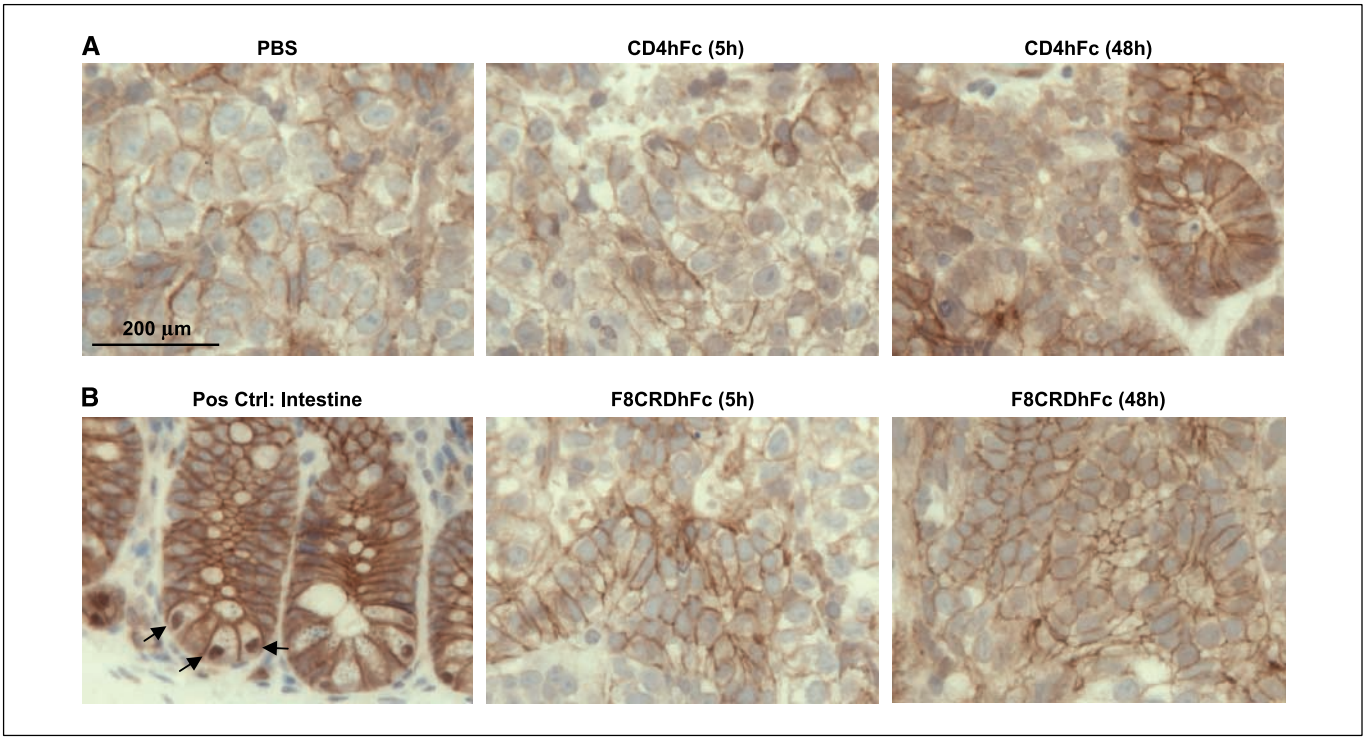

Figure 4. Effect of F8CRDhFc administration on β-catenin localization in NTera-2 tumor xenografts harvested from mice treated with a single dose of the indicated agent for either 5 or 48 h. Immunohistochemistry staining shows nuclear β-catenin localization in Paneth cells of the small intestine (*arrowheads, bottom left*). *Bar,* 200 μm.

tumor model after 14 treatments, thrice a week, and sections were stained for β-catenin protein by immunohistochemistry. Analysis of skin and various intestinal compartments revealed that the architecture of these tissues appeared morphologically normal in treated mice of all groups, with typical patterns of cytoplasmic and nuclear β-catenin staining in intestinal Paneth cells (Fig. 6*A*) and skin hair follicles (Fig. 6*B*). Furthermore, histologic and immunohistochemical analysis of skin and intestine collected from animals using the NTera-2 model, after nine treatments, thrice a week also revealed no differences between control and treated groups (data not shown). This suggests that treatment with F8CRDhFc with the therapeutic regimen that can inhibit tumor growth does not have adverse effects on tissue renewal of skin and intestine.

Discussion

The evidence for dysregulated wnt signaling in cancer is readily apparent from genetic defects identified in pathway components. It is therefore reasonable to presume that epigenetic mechanisms resulting in hyperactive wnt signaling might also contribute to human cancer progression. Numerous studies have associated the overexpression of wnt ligands and their receptors, or down-regulation of wnt antagonists such as sFRP, Dkk1, and WIF-1, with the occurrence of cancer. Based on these observations, it has been suggested that molecules which interfere with wnt ligand/receptor interactions might be useful as therapeutic agents in these cancers. Several approaches such as the use of monoclonal antibodies against wnt ligands (24, 25) and overexpression of wnt antagonists in tumor cells (14, 26, 27) have shown that inhibition of wnt signaling can reduce *in vivo* tumor growth.

We have generated a novel form of a soluble wnt receptor, F8CRDhFc, which exhibits favorable pharmacologic behavior *in vivo*. Using the MMTV-Wnt1 tumor model, we showed that F8CRDhFc treatment results in the regression of established wnt1-driven tumors, clearly showing the *in vivo* potency of the F8CRDhFc-soluble receptor. The tumor inhibition was reversible in this model as regrowth was observed after F8CRDhFc dosing was discontinued. This is consistent with studies in which mammary tumor growth and regression correlated with the expression status of the conditional wnt1 transgene (9). To validate the utility of F8CRDhFc in human cancers, we identified tumorigenic cell lines that exhibited endogenous wnt ligand–driven signaling. Some human germ cell tumors (42) and cell lines derived from these tumors have increased basal wnt signaling (14) and show a canonical response to stimulation and inhibition of wnt signaling (14, 43). We screened the teratoma cell lines NTera-2, Tera-2, and NCCIT for increased basal wnt signaling activity and showed that, similar to PA-1 cells (14), treatment with F8CRDhFc could inhibit this activity *in vitro*. Nevertheless, it was not clear that this wnt activity contributed to the tumorigenic potential of these cancer cell lines. Using model systems with xenograft tumors derived from NTera-2 and PA-1 cells, we have shown that administration of therapeutic doses of F8CRDhFc results in a significant suppression of these tumors as well. A molecular diagnostic marker for wnt signaling will be essential to identify human cancers that are amenable to treatment with F8CRDhFc. Although the cell lines screened have up-regulated wnt signaling, immunohistochemical analysis of β-catenin localization in the corresponding tumors was not a reliable indicator of this activity (Supplementary Fig. S2). This could be a distinction between cells that have autocrine wnt signaling compared with cells harboring APC or β-catenin mutations. Accordingly, it has been shown that increased nuclear β-catenin in ovarian carcinoma is specifically associated with β-catenin mutations (44). Immunohistochemical

analysis of xenograft tissue from F8CRDhFc-treated mice in the MMTV-Wnt1 and NTera-2 tumors did not show differences in the levels or cellular localization of β-catenin, suggesting that changes in β-catenin may be too small to detect. Similarly, expression of the CRD of Fzd7 did not affect β-catenin levels or localization, although tumor growth was reduced (26).

As an alternative to immunohistochemical analysis of β-catenin, we identified transcriptional targets of wnt to monitor signaling activity and drug response. The cell lines that had autocrine wnt signaling showed increased expression of known wnt target genes and this expression was regulated by *in vitro* treatment with wnt3a as well as by F8CRDhFc. Although tumors derived from NTera-2 cells did not show any changes in β-catenin on F8CRDhFc treatment, RNA analysis of these samples revealed that F8CRDhFc treatment does affect expression of the wnt target genes tested. Thus, the expression of these genes can be followed as an indicator of treatment efficacy. As an extension of these observations, expression of these wnt target genes can be used as a diagnostic tool to identify cancers that are driven by wnt signaling and are therefore candidates for anti-wnt therapeutic agents.

Several studies suggest that inhibition of wnt signaling could adversely affect the architecture of the skin (45) and intestine

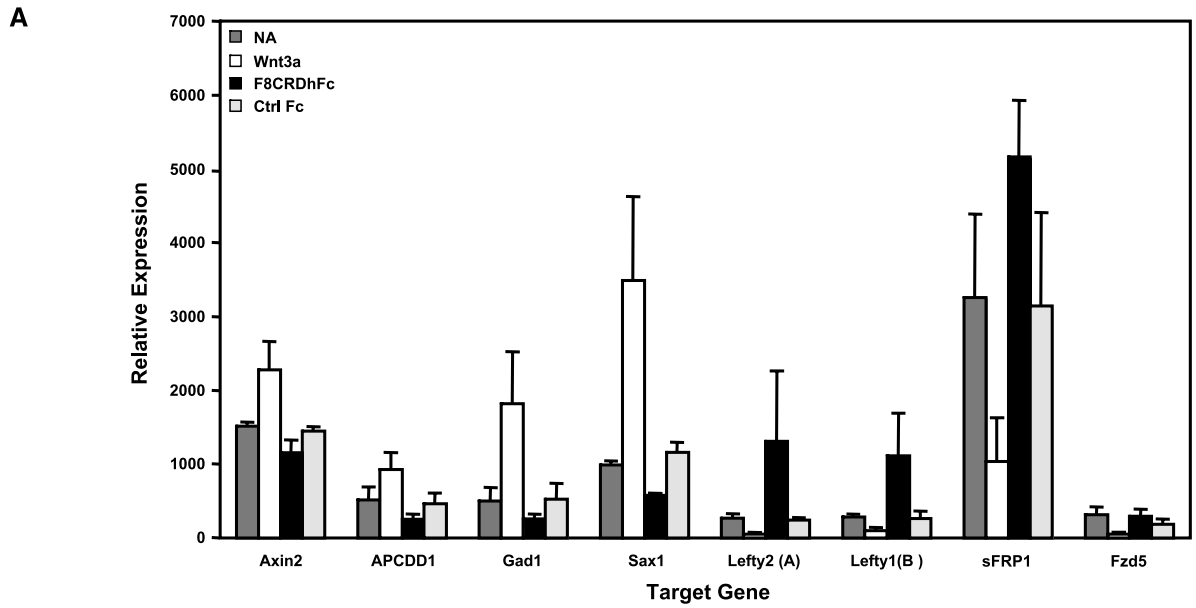

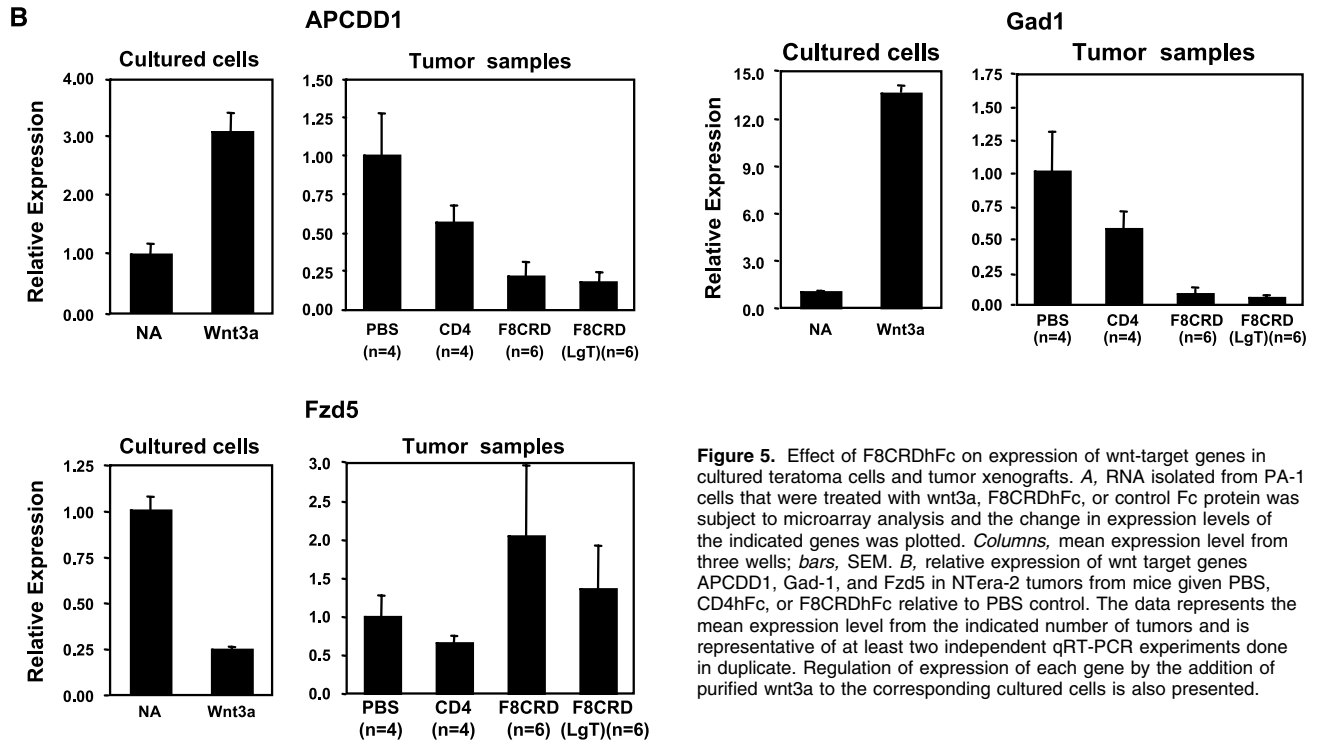

Figure 5. Effect of F8CRDhFc on expression of wnt-target genes in cultured teratoma cells and tumor xenografts. *A,* RNA isolated from PA-1 cells that were treated with wnt3a, F8CRDhFc, or control Fc protein was subject to microarray analysis and the change in expression levels of the indicated genes was plotted. *Columns,* mean expression level from three wells; *bars,* SEM. *B,* relative expression of wnt target genes APCDD1, Gad-1, and Fzd5 in NTera-2 tumors from mice given PBS, CD4hFc, or F8CRDhFc relative to PBS control. The data represents the mean expression level from the indicated number of tumors and is representative of at least two independent qRT-PCR experiments done in duplicate. Regulation of expression of each gene by the addition of purified wnt3a to the corresponding cultured cells is also presented.

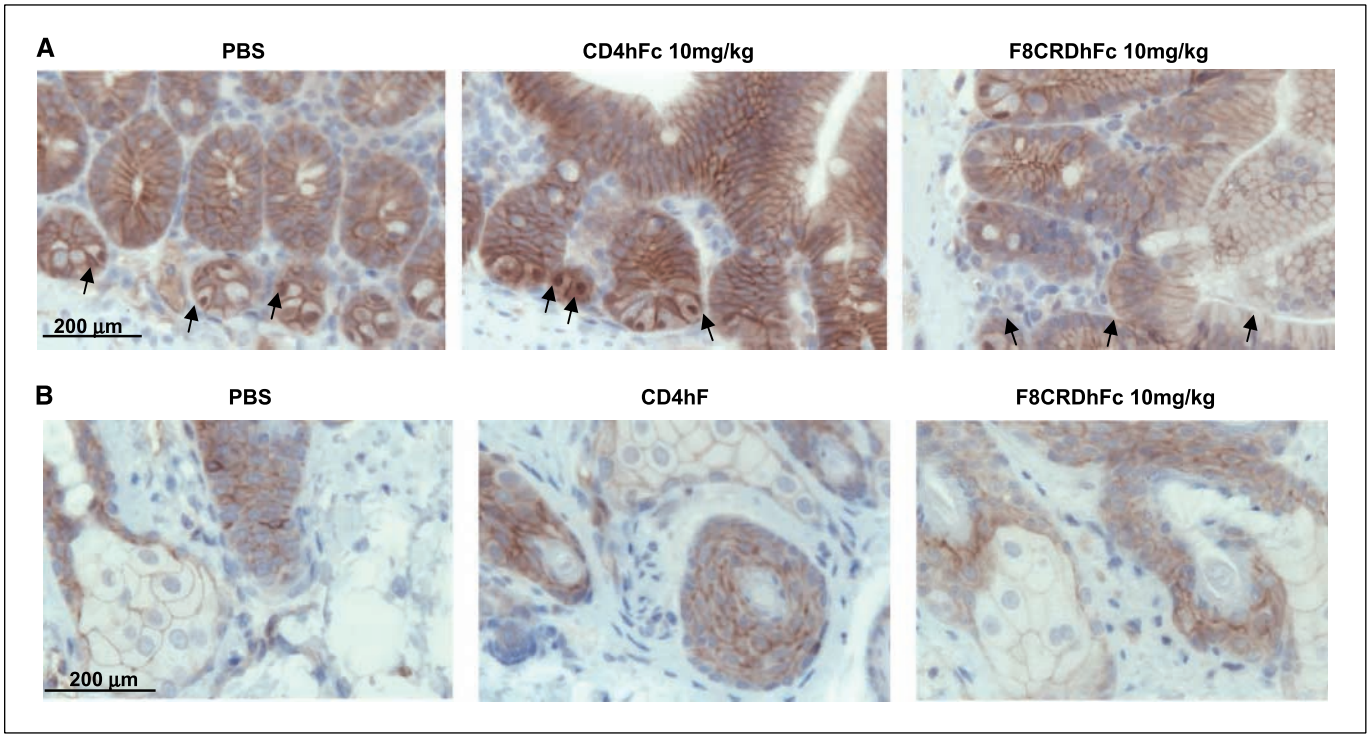

Figure 6. Histologic examination of intestine and skin for adverse effects of F8CRDhFc. Immunohistochemistry staining for β-catenin in small intestine (*A*) and skin (*B*) of mice treated with PBS, CD4hFc, and F8CRDhFc. *A,* Paneth cells at the base of the crypts (*arrows*). All tissue samples were collected from mice treated following an efficacy study using the MMTV-Wnt1 model after 14 treatments with the indicated agent thrice a week. *Bar,* 200 μm.

(40, 41). This is presumably linked to an important role for wnt in the maintenance of stem cells that play a critical role in the regeneration of these tissue compartments. In our studies, mice treated with F8CRDhFc seemed healthy and showed no dramatic weight loss, suggesting that the molecule had limited overall toxicity. Histologic analysis showed that skin and intestine of F8CRDhFc-treated mice were normal, with typical patterns of cytoplasmic and nuclear β-catenin staining in intestinal Paneth cells and skin hair follicles. The published reports showing the adverse effects of inhibiting wnt signaling in the intestine used either adenoviral-mediated expression (40) or tissue-specific transgenic expression (41) of Dkk1. It is possible that the local or high-level expression of wnt antagonist achieved in these studies greatly exceeded the therapeutic dose of inhibitor administered in our studies. Alternately, both Dkk1 and F8CRDhFc inhibit wnt signaling by distinct mechanisms and they may have different effects on intestine *in vivo*.

Our choice of teratomas for testing the therapeutic effect of F8CRDhFc was based on the presence of autocrine wnt signal detected in these cells when cultured *in vitro*. However, cancer cell lines lacking this property might nevertheless express wnts when grown *in vivo* or respond to wnt ligands supplied by host stromal cells and thereby respond to inhibition by F8CRDhFc. A broader understanding of which human cancers are amenable to treatment with F8CRDhFc will be required to determine the overall breadth of its utility in this disease. Human breast cancers represent an attractive candidate for F8CRDhFc therapy, as there is substantial evidence for abnormal wnt signaling, yet mutations in wnt pathway components are rare (46). It also remains possible that cancers containing mutations in downstream wnt pathway genes still rely on wnt ligands for tumorigenicity, and consistent with this, epigenetic silencing of genes coding for the sFRPs has been observed in colorectal cancer (20). Although we have found no effect of purified F8CRDhFc, sFRP1, or Dkk1 on wnt signaling *in vitro* in colorectal cancer cells containing pathway mutations (data not shown), wnt ligands might contribute to their tumorigenicity in a manner not measurable with synthetic wnt reporter plasmids. For example, wnt ligands can activate the growth control pathways mediated by mTOR-S6 kinase (47), Akt (48), and ERK (49) through β-catenin–independent mechanisms.

In conclusion, we have used both an engineered tumor model as well as naturally occurring models with autocrine wnt signaling to show that wnt signaling can be modulated in a pharmacologically relevant manner *in vivo* by F8CRDhFc. Although the wnt pathway has been implicated in many cancers, it is not clear which of the 21 known wnt ligands play a role in human cancer. The Fzd CRD domains identified thus far share significant sequence similarity and proposed structure (50), strongly suggesting that most of these domains may share a common biological function in binding wnt ligands. The F8CRDhFc molecule described here is predicted to bind to and inhibit the activity of multiple wnt ligands and may therefore be efficacious in inhibiting the growth of tumors driven by multiple wnt or Fzd homologues.

Acknowledgments

Received 1/22/2007; revised 3/2/2007; accepted 3/27/2007.

The costs of publication of this article were defrayed in part by the payment of page charges. This article must therefore be hereby marked *advertisement* in accordance with 18 U.S.C. Section 1734 solely to indicate this fact.

Our thanks to Michelle Simpson, Hong Li, and Phil Hass for protein purification, Kristen Harden for Biacore studies, Karen Billeci for ELISA assays, David Petersen and David Dornan for U2OS assays, Arthur Reyes for pharmacokinetic studies, Noelyn Kljavin for animal studies, Fiona Zhong and Sheila Bheddah for immunohistochemistry, Grazyna Fedorowicz, Zora Modrusan, and Tom Wu for microarray analysis, and the animal husbandry and necropsy groups for technical assistance.

References

1. Clevers H. Wnt/β-catenin signaling in development and disease. Cell 2006;127:469–80.
2. Willert K, Jones KA. Wnt signaling: is the party in the nucleus? Genes Dev 2006;20:1394–404.
3. Cadigan KM, Nusse R. Wnt signaling: a common theme in animal development. Genes Dev 1997;11: 3286–305.
4. Reya T, Clevers H. Wnt signalling in stem cells and cancer. Nature 2005;434:843–50.
5. Nusse R, Varmus HE. Many tumors induced by the mouse mammary tumor virus contain a provirus integrated in the same region of the host genome. Cell 1982;31:99–109.
6. Tsukamoto AS, Grosschedl R, Guzman RC, Parslow T, Varmus HE. Expression of the int-1 gene in transgenic mice is associated with mammary gland hyperplasia and adenocarcinomas in male and female mice. Cell 1988;55:619–25.
7. Fuchs SY, Ougolkov AV, Spiegelman VS, Minamoto T. Oncogenic β-catenin signaling networks in colorectal cancer. Cell Cycle 2005;4:1522–39.
8. Ilyas M. Wnt signalling and the mechanistic basis of tumour development. J Pathol 2005;205:130–44.
9. Gunther EJ, Moody SE, Belka GK, et al. Impact of p53 loss on reversal and recurrence of conditional Wnt-induced tumorigenesis. Genes Dev 2003;17:488–501.
10. Polakis P. Wnt signaling and cancer. Genes Dev 2000; 14:1837–51.
11. Polakis P. The many ways of Wnt in cancer. Curr Opin Genet Dev 2007;17:45–51.
12. Holcombe RF, Marsh JL, Waterman ML, Lin F, Milovanovic T, Truong T. Expression of Wnt ligands and Frizzled receptors in colonic mucosa and in colon carcinoma. Mol Pathol 2002;55:220–6.
13. Huguet EL, McMahon JA, McMahon AP, Bicknell R, Harris AL. Differential expression of human Wnt genes 2, 3, 4, and 7B in human breast cell lines and normal and disease states of human breast tissue. Cancer Res 1994; 54:2615–21.
14. Bafico A, Liu G, Goldin L, Harris V, Aaronson SA. An autocrine mechanism for constitutive Wnt pathway activation in human cancer cells. Cancer Cell 2004;6: 497–506.
15. Zeng G, Germinaro M, Micsenyi A, et al. Aberrant Wnt/β-catenin signaling in pancreatic adenocarcinoma. Neoplasia 2006;8:279–89.
16. Janssens N, Andries L, Janicot M, Perera T, Bakker A. Alteration of frizzled expression in renal cell carcinoma. Tumour Biol 2004;25:161–71.
17. Hoang BH, Kubo T, Healey JH, et al. Expression of LDL receptor-related protein 5 (LRP5) as a novel marker for disease progression in high-grade osteosarcoma. Int J Cancer 2004;109:106–11.
18. Li Y, Lu W, He X, Schwartz AL, Bu G. LRP6 expression promotes cancer cell proliferation and tumorigenesis by altering β-catenin subcellular distribution. Oncogene 2004;23:9129–35.
19. Taniguchi H, Yamamoto H, Hirata T, et al. Frequent epigenetic inactivation of Wnt inhibitory factor-1 in human gastrointestinal cancers. Oncogene 2005;24: 7946–52.
20. Suzuki H, Watkins DN, Jair KW, et al. Epigenetic inactivation of SFRP genes allows constitutive WNT signaling in colorectal cancer. Nat Genet 2004;36: 417–22.
21. Veeck J, Niederacher D, An H, et al. Aberrant methylation of the Wnt antagonist SFRP1 in breast cancer is associated with unfavourable prognosis. Oncogene 2006;25:3479–88.
22. Aguilera O, Fraga MF, Ballestar E, et al. Epigenetic inactivation of the Wnt antagonist DICKKOPF-1 (DKK-1) gene in human colorectal cancer. Oncogene 2006;25:4116–21.
23. Kawano Y, Kypta R. Secreted antagonists of the Wnt signalling pathway. J Cell Sci 2003;116:2627–34.
24. He B, You L, Uematsu K, et al. A monoclonal antibody against Wnt-1 induces apoptosis in human cancer cells. Neoplasia 2004;6:7–14.
25. You L, He B, Xu Z, et al. An anti-Wnt-2 monoclonal antibody induces apoptosis in malignant melanoma cells and inhibits tumor growth. Cancer Res 2004;64: 5385–9.
26. Vincan E, Darcy PK, Smyth MJ, et al. Frizzled-7 receptor ectodomain expression in a colon cancer cell line induces morphological change and attenuates tumor growth. Differentiation 2005;73:142–53.
27. Zi X, Guo Y, Simoneau AR, et al. Expression of Frzb/ secreted Frizzled-related protein 3, a secreted Wnt antagonist, in human androgen-independent prostate cancer PC-3 cells suppresses tumor growth and cellular invasiveness. Cancer Res 2005;65:9762–70.
28. Capon DJ, Chamow SM, Mordenti J, et al. Designing CD4 immunoadhesins for AIDS therapy. Nature 1989; 337:525–31.
29. Harris RJ, Wagner KL, Spellman MW. Structural characterization of a recombinant CD4-IgG hybrid molecule. Eur J Biochem 1990;194:611–20.
30. Willert K, Brown JD, Danenberg E, et al. Wnt proteins are lipid-modified and can act as stem cell growth factors. Nature 2003;423:448–52.
31. Chen Y, Wiesmann C, Fuh G, et al. Selection and analysis of an optimized anti-VEGF antibody: crystal structure of an affinity-matured Fab in complex with antigen. J Mol Biol 1999;293:865–81.
32. Rubinfeld B, Upadhyay A, Clark SL, et al. Identification and immunotherapeutic targeting of antigens induced by chemotherapy. Nat Biotechnol 2006;24:205–9.
33. Jubb AM, Chalasani S, Frantz GD, et al. Achaete-scute like 2 (ascl2) is a target of Wnt signalling and is upregulated in intestinal neoplasia. Oncogene 2006;25: 3445–57.
34. Hsieh JC, Rattner A, Smallwood PM, Nathans J. Biochemical characterization of Wnt-frizzled interactions using a soluble, biologically active vertebrate Wnt protein. Proc Natl Acad Sci U S A 1999;96:3546–51.
35. Reya T, Duncan AW, Ailles L, et al. A role for Wnt signalling in self-renewal of haematopoietic stem cells. Nature 2003;423:409–14.
36. Dann CE, Hsieh JC, Rattner A, Sharma D, Nathans J, Leahy DJ. Insights into Wnt binding and signalling from the structures of two Frizzled cysteine-rich domains. Nature 2001;412:86–90.
37. Yan D, Wiesmann M, Rohan M, et al. Elevated expression of axin2 and hnkd mRNA provides evidence that Wnt/β-catenin signaling is activated in human colon tumors. Proc Natl Acad Sci U S A 2001;98:14973–8.
38. Zirn B, Samans B, Wittmann S, et al. Target genes of the WNT/β-catenin pathway in Wilms tumors. Genes Chromosomes Cancer 2006;45:565–74.
39. Li CM, Kim CE, Margolin AA, et al. CTNNB1 mutations and overexpression of Wnt/β-catenin target genes in WT1-mutant Wilms' tumors. Am J Pathol 2004; 165:1943–53.
40. Kuhnert F, Davis CR, Wang HT, et al. Essential requirement for Wnt signaling in proliferation of adult small intestine and colon revealed by adenoviral expression of Dickkopf-1. Proc Natl Acad Sci U S A 2004;101:266–71.
41. Pinto D, Gregorieff A, Begthel H, Clevers H. Canonical Wnt signals are essential for homeostasis of the intestinal epithelium. Genes Dev 2003;17:1709–13.
42. Fritsch MK, Schneider DT, Schuster AE, Murdoch FE, Perlman EJ. Activation of Wnt/β-catenin signaling in distinct histologic subtypes of human germ cell tumors. Pediatr Dev Pathol 2006;9:115–31.
43. Willert J, Epping M, Pollack JR, Brown PO, Nusse R. A transcriptional response to Wnt protein in human embryonic carcinoma cells. BMC Dev Biol 2002;2:8.
44. Sarrio D, Moreno-Bueno G, Sanchez-Estevez C, et al. Expression of cadherins and catenins correlates with distinct histologic types of ovarian carcinomas. Hum Pathol 2006;37:1042–9.
45. Merrill BJ, Gat U, DasGupta R, Fuchs E. Tcf3 and Lef1 regulate lineage differentiation of multipotent stem cells in skin. Genes Dev 2001;15:1688–705.
46. Howe LR, Brown AM. Wnt signaling and breast cancer. Cancer Biol Ther 2004;3:36–41.
47. Inoki K, Ouyang H, Zhu T, et al. TSC2 integrates Wnt and energy signals via a coordinated phosphorylation by AMPK and GSK3 to regulate cell growth. Cell 2006;126: 955–68.
48. Kim SE, Lee WJ, Choi KY. The PI3 kinase-Akt pathway mediates Wnt3a-induced proliferation. Cell Signal 2006;19:511–8.
49. Yun MS, Kim SE, Jeon SH, Lee JS, Choi KY. Both ERK and Wnt/β-catenin pathways are involved in Wnt3a-induced proliferation. J Cell Sci 2005;118:313–22.
50. Wang HY, Liu T, Malbon CC. Structure-function analysis of Frizzleds. Cell Signal 2006;18:934–41.

The Soluble Wnt Receptor Frizzled8CRD-hFc Inhibits the Growth of Teratocarcinomas *In vivo*

Venita I. DeAlmeida, Li Miao, James A. Ernst, et al.

Cancer Res 2007;67:5371-5379.